Noise on photon correlation data. I. Autocorrelation functions

1990 Quantum Opt. 2 287

(http://iopscience.iop.org/0954-8998/2/4/002)

Quantum Opt. 2 (1990) 287–305. Printed in the UK

Noise on photon correlation data: I. Autocorrelation functions

Klaus Schätzel

Institut für Angewandte Physik der Universität Kiel, Kiel, D-2300, Federal Republic of Germany

Received 6 December 1989, in final form 13 February 1990

Abstract. An adequate analysis of photon correlation data requires knowledge about the statistical accuracy of the measured data. For the model of gamma-distributed intensities, that is including the effect of a finite intercept, the full covariance matrix is calculated for all the channels of the photon autocorrelation functions. A thorough discussion of multiple sample time correlation illuminates the importance of temporal averaging effects at large lag times. A practical estimation scheme is given for the noise in photon correlation data from a multiple sample time measurement.

1. Introduction

Photon correlation spectroscopy, the digital correlation of single-photon detection events, provides a powerful technique for time domain spectroscopy at low light levels. The range of possible applications is still growing, most notably in the field of dynamic light scattering from colloidal systems [1]. After the two initial generations of digital correlators, which provided single-bit and subsequently multi-bit processing at a single sampling time, a third generation of correlator hardware is now commercially available, where sampling at multiple sample times provides simultaneous correlation data over very large lag time ranges.

The accuracy of photon correlation measurements was computed by several authors soon after the introduction of this technique about 1970 [2, 3, 4]. However, these computations were limited to Gaussian statistics of the scattered light amplitude and the case of autocorrelation functions measured at a single sample time. Furthermore, the only paper giving a full covariance matrix for the measured autocorrelation function [4], unfortunately contains a number of errors [5].

Hence, a more extensive treatment of noise on photon correlation data is highly desirable and is in fact a necessity, because modern inversion programs (for example, CONTIN [6] or maximum-entropy analysis [7]) for the analysis of measured correlation functions require precise noise estimates in order to achieve optimum performance.

This paper presents the complete calculation of the full covariance matrix of real-time correlation measurements for the rather general case of gamma intensity statistics, that is including the common feature of reduced intercept. Special attention is given to correlation functions measured with different simultaneous sample times, in particular the 'multiple-tau' scheme recently implemented in hardware correlators [8]. An

0954-8998/90/040287 + 19 $3.50

extension of these calculations to cross-correlation functions is under preparation for future publication.

2. Correlation at a single sample time

2.1. Photon correlation

Photon counting detection of light requires the introduction of a sample time t_s during which incoming photon detection pulses are summed. For maximum counting efficiency, the stop time of a particular sample time interval should coincide with the start time of the subsequent interval. As a result, we obtain a sequence of pulse counts denoted as

$$n_i \qquad i = 1, 2, 3, \ldots . \tag{1}$$

Ignoring instrumental distortions like afterpulsing or dead time [9, 10], photon counting events can be regarded as statistically independent point events and a Poisson distribution must be expected for the n_i with a mean value given by the classical light intensity $I(t)$ integrated over the particular sample time interval i under consideration [11]. We shall denote this integrated intensity as

$$\mu_i = \int_{(i-1)t_s}^{it_s} I(t)\,\mathrm{d}t \qquad i = 1, 2, 3, \ldots \tag{2}$$

where we absorb irrelevant factors like the quantum efficiency of the detector into our intensity unit.

The digital correlation of equation (1) results in an estimator for the temporal autocorrelation function of photon counts—in short, the photon correlation function—

$$\hat{G}_n(k) = \frac{1}{M}\sum_{i=1}^{M} n_i n_{i+k} \qquad k = 1, 2, 3, \ldots . \tag{3}$$

It must be pointed out, that this estimator is not the only possible choice. In principle, the index i could be stepped by increments larger than 1 or even using unequal steps (batch processing), in order to reduce the requirements in terms of computational power of the correlator. However, our scheme is the most efficient one in terms of statistical accuracy for a given total duration of the measurement and is in fact realized for the real-time digital correlators referred to in this paper.

A quick calculation proves the well known fact that the expectation value of equation (3) essentially equals the corresponding intensity correlation function for all non-zero k:

$$\langle \hat{G}_n(k) \rangle = \langle n_i n_{i+k} \rangle = \langle \mu_i \mu_{i+k} \rangle = \int_{-t_s}^{t_s} \langle I(0) I(kt_s + t) \rangle (t_s - |t|)\,\mathrm{d}t. \tag{4}$$

In equation (4) we assume stationarity for $I(t)$, which is now treated as a stochastic process. If our sample time t_s is well below the time scale of typical fluctuations in $I(t)$, that is the coherence time t_c, we may simply ignore the narrow triangular average in the final expression of equation (4) and obtain the familiar relation

$$\langle \hat{G}_n(k) \rangle = \langle n_i n_{i+k} \rangle \approx t_s^2 \langle I(0) I(kt_s) \rangle . \tag{5}$$

However, in the context of multiple sample time correlation, we shall later have to relax this requirement of short sample times.

2.2 *Normalization*

Typical applications of photon correlation spectroscopy evaluate the shape of measured correlation functions rather than their absolute magnitude. Normalization by the square of the measured count rate per sample time,

$$\hat{n} = M^{-1} \sum_{i=1}^{M} n_i \tag{6}$$

leads to a normalized correlation estimator

$$\hat{g}_n(k) = \hat{G}_n(k)/\hat{n}^2 - 1. \tag{7}$$

It is well known that this normalization reduces estimator noise by partial cancellation of fluctuations in the unnormalized correlation estimator and the count rate estimator, but does also introduce some bias [12].

At large lag times, the normalization procedure may be improved by the use of a second, lag-time-specific monitor channel

$$\hat{n}_k = M^{-1} \sum_{i=1}^{M} n_{i+k} \tag{8}$$

which allows symmetric normalization

$$\hat{g}_n^{(s)}(k) = \hat{G}_n(k)/\hat{n}_0\hat{n}_k - 1 \tag{9}$$

to be applied [13]. The symmetric normalization scheme reduces estimator noise by cancellation of contributions due to boundary terms, that is terms involving just the first or the last k samples of a data set. For most of the following calculations we shall ignore the difference between equations (7) and (9), since it is of order k/M, only.

In order to avoid complications due to the occurrence of an estimator in the denominator in equation (7), we follow the usual approach and replace this estimator by the sum of its expectation and its (small) fluctuation about the mean:

$$\hat{n} = \bar{n} + \delta\hat{n}. \tag{10}$$

Expanding the denominator in equation (7) we obtain

$$\hat{g}_n(k) = \bar{n}^{-2}\hat{G}_n(k)(1 - 2\delta\hat{n}/\bar{n} + 3\delta\hat{n}^2/\bar{n}^2 - \ldots) - 1. \tag{11}$$

2.3. *Photon statistics*

The first steps of our calculation do not yet require full knowledge of the intensity statistics. For any given time-integrated intensities μ_i we obtain the well known Poisson moments [11]

$$\langle n_i | \mu_i \rangle = \mu_i \tag{12}$$

$$\langle n_i n_j | \mu_i, \mu_j \rangle = \mu_i\mu_j + \delta_{ij}\mu_i \tag{13}$$

$$\langle n_i n_j n_m | \mu_i, \mu_j, \mu_m \rangle = \mu_i\mu_j\mu_m + \delta_{ij}\mu_i\mu_m + \delta_{im}\mu_i\mu_j + \delta_{jm}\mu_i\mu_j + \delta_{ij}\delta_{im}\mu_i \tag{14}$$

$$\begin{aligned}\langle n_i n_j n_m n_p | \mu_i, \mu_j, \mu_m, \mu_p \rangle = {} & \mu_i\mu_j\mu_m\mu_p + \delta_{ij}\mu_i\mu_m\mu_p + \delta_{im}\mu_i\mu_j\mu_p \\ & + \delta_{ip}\mu_i\mu_j\mu_m + \delta_{jm}\mu_i\mu_j\mu_p + \delta_{jp}\mu_i\mu_j\mu_m + \delta_{mp}\mu_i\mu_j\mu_m \\ & + \delta_{ij}\delta_{im}\mu_i\mu_p + \delta_{ij}\delta_{ip}\mu_i\mu_m + \delta_{im}\delta_{ip}\mu_i\mu_j + \delta_{jm}\delta_{jp}\mu_i\mu_j \\ & + \delta_{ij}\delta_{mp}\mu_i\mu_m + \delta_{im}\delta_{jp}\mu_i\mu_j + \delta_{ip}\delta_{jm}\mu_i\mu_j + \delta_{ij}\delta_{im}\delta_{ip}\mu_i. \end{aligned} \tag{15}$$

From these conditional moments we calculate some covariances, ignoring terms beyond order M^{-1} and using stationarity of the μ_i:

$$\begin{aligned}\operatorname{cov}(\hat{G}_n(k), \hat{G}_n(l)) = {} & M^{-2} \sum_{i,j=1}^{M} \langle \mu_i \mu_{i+k} \mu_j \mu_{j+l} \rangle - \langle \mu_0\mu_k \rangle \langle \mu_0\mu_l \rangle \\ & + M^{-1}(\langle \mu_0\mu_k\mu_l \rangle + \langle \mu_0\mu_k\mu_{k+l} \rangle + \langle \mu_0\mu_l\mu_{k+l} \rangle \\ & + \langle \mu_0\mu_{k-l}\mu_k \rangle + \delta_{k\backslash}\langle \mu_0\mu_k \rangle) \end{aligned} \tag{16}$$

$$\operatorname{cov}(\hat{G}_n(k), \hat{n}) = M^{-2} \sum_{i,j=1}^{M} \langle \mu_i \mu_{i+k} \mu_j \rangle - \langle \mu_0\mu_k \rangle \bar{n} + 2M^{-1}\langle \mu_0\mu_k \rangle, \tag{17}$$

$$\operatorname{var}(\hat{n}) = M^{-2} \sum_{i,j=1}^{M} \langle \mu_i \mu_j \rangle - \bar{n}^2 + M^{-1}\bar{n}. \tag{18}$$

$\bar{n}$ denotes the expectation value of μ_i and agrees with our earlier definition given by equation (10).

It is now a simple task to compute the expectation value of our normalized estimator, again up to order M^{-1}:

$$\begin{aligned}\langle \hat{g}_n(k) \rangle = {} & \bar{n}^{-2}\langle \mu_0\mu_k \rangle - 2\bar{n}^{-3} \operatorname{cov}(\hat{G}_n(k), \hat{n}) + 3\bar{n}^{-4}\langle \mu_0\mu_k \rangle \operatorname{var}(n) - 1 \\ = {} & \bar{n}^{-2}\langle \mu_0\mu_k \rangle - 2\bar{n}^{-3}\left(M^{-2} \sum_{i,j=1}^{M} \langle \mu_i\mu_{i+k}\mu_j \rangle - \langle \mu_0\mu_k \rangle \bar{n} + 2M^{-1}\langle \mu_0\mu_k \rangle \right) \\ & + 3\bar{n}^{-4}\langle \mu_0\mu_k \rangle \left(M^{-2} \sum_{i,j=1}^{M} \langle \mu_i\mu_j \rangle - \bar{n}^2 + M^{-1}\bar{n} \right) - 1 \\ = {} & \bar{n}^{-2}\langle \mu_0\mu_k \rangle + M^{-1}\bar{n}^{-4}\left(3\langle \mu_0\mu_k \rangle \sum_i (\langle \mu_0\mu_i \rangle - \bar{n}^2) \right. \\ & \left. - 2\bar{n} \sum_i (\langle \mu_0\mu_k\mu_i \rangle - \langle \mu_0\mu_k \rangle \bar{n}) - \bar{n}\langle \mu_0\mu_k \rangle \right) - 1. \end{aligned} \tag{19}$$

The sum index i is understood to run from large negative to large positive values. A finite correlation time of the μ_i, which is short compared to the total measurement time Mt_s, will ensure convergence of all the summations in equation (19), and, once again, keep errors in this equation below the order M^{-1}.

Obviously, we may neglect the bias terms in equation (19) if Mt_s is large compared with the correlation time t_c and if M is a large number itself. These conditions hold true for most real photon correlation experiments, except at very large lag and sample times.

In order to calculate noise estimates accurate to the order M^{-1}, we may truncate our expression, equation (11), for the normalized correlation estimator at the first-order term and obtain

$$\begin{aligned}\operatorname{cov}(\hat{g}_n(k), \hat{g}_n(l)) &= \bar{n}^{-4}\operatorname{cov}(\hat{G}_n(k), \hat{G}_n(l)) - 2\bar{n}^{-5}\langle\hat{G}_n(k)\rangle\operatorname{cov}(\hat{G}_n(l), \hat{n}) \\ &\quad - 2\bar{n}^{-5}\langle\hat{G}_n(l)\rangle\operatorname{cov}(\hat{G}_n(k), \hat{n}) + 4\bar{n}^{-6}\langle\hat{G}_n(k)\rangle\langle\hat{G}_n(l)\rangle\operatorname{var}(\hat{n}) \\ &= \operatorname{cov}(\hat{g}_\mu(k), \hat{g}_\mu(l)) + M^{-1}\bar{n}^{-4}(\langle\mu_0\mu_k\mu_l\rangle + \langle\mu_0\mu_k\mu_{k+l}\rangle \\ &\quad + \langle\mu_0\mu_l\mu_{k+l}\rangle + \langle\mu_0\mu_{k-l}\mu_k\rangle - 4\langle\mu_0\mu_k\rangle\langle\mu_0\mu_l\rangle/\bar{n} + \delta_{kl}\langle\mu_0\mu_k\rangle). \qquad (20)\end{aligned}$$

In equation (20) we have introduced the normalized estimator for the correlation of the temporally integrated intensities μ_i,

$$\hat{g}_\mu(k) = \hat{G}_\mu(k)/\hat{\mu}^2 - 1 = \bar{n}^{-2}\hat{G}_\mu(k)[1 - 2\delta\hat{n}/\bar{n} + 3(\delta\hat{n}/\bar{n})^2 - \ldots] - 1 \qquad (21)$$

with

$$\hat{\mu} = M^{-1}\sum_{i=1}^{M}\mu_i \qquad \delta\hat{\mu} = \hat{\mu} - \bar{n} \qquad \hat{G}_\mu(k) = M^{-1}\sum_{i=1}^{M}\mu_i\mu_{i+k} \qquad (22)$$

leading to

$$\begin{aligned}\operatorname{cov}(\hat{g}_\mu(k), \hat{g}_\mu(l)) &= \bar{n}^{-4}\operatorname{cov}(\hat{G}_\mu(k), \hat{G}_\mu(l)) \\ &\quad - 2\bar{n}^{-5}[\langle\hat{G}_\mu(k)\rangle\operatorname{cov}(\hat{G}_\mu(l), \delta\hat{\mu}) + \langle\hat{G}_\mu(l)\rangle\operatorname{cov}(\hat{G}_\mu(k), \delta\hat{\mu})] \\ &\quad + 4\bar{n}^{-6}\langle\hat{G}_\mu(k)\rangle\langle\hat{G}_\mu(l)\rangle\operatorname{var}(\delta\hat{\mu}) + \mathrm{O}(M^{-2}) \\ &= \bar{n}^{-4}M^{-2}\sum_{i,j=1}^{M}(\langle\mu_i\mu_{i+k}\mu_j\mu_{j+l}\rangle - \langle\mu_0\mu_k\rangle\langle\mu_0\mu_l\rangle) - 2\bar{n}^{-5}M^{-2} \\ &\quad \times \sum_{i,j=1}^{M}[\langle\mu_0\mu_k\rangle(\langle\mu_i\mu_{i+l}\mu_j\rangle - \langle\mu_0\mu_l\rangle\bar{n}) + \langle\mu_0\mu_l\rangle(\langle\mu_i\mu_{i+k}\mu_j\rangle - \langle\mu_0\mu_k\rangle\bar{n})] \\ &\quad + 4\bar{n}^{-6}M^{-2}\langle\mu_0\mu_k\rangle\langle\mu_0\mu_l\rangle\sum_{i,j=1}^{M}(\langle\mu_i\mu_j\rangle - \bar{n}^2) + \mathrm{O}(M^{-2}). \qquad (23)\end{aligned}$$

Please note that, due to the decrease in correlations with lag time, all double summations only contribute for index values i and j that do not differ by much more than the ratio of coherence time to sample time. Hence all terms are really of order $1/M$ only, as was to be expected. For the typical case of total measurement times much larger than the coherence time and stationary μ_i, we may further replace the double summations by a single summation over all values of the difference of i and j and obtain to order $1/M$

$$\begin{aligned}\operatorname{cov}(\hat{g}_\mu(k), \hat{g}_\mu(l)) &= M^{-1}\bar{n}^{-4}\Bigg(\sum_i(\langle\mu_0\mu_k\mu_i\mu_{i+l}\rangle - \langle\mu_0\mu_k\rangle\langle\mu_0\mu_l\rangle) \\ &\quad - 2\langle\mu_0\mu_k\rangle\sum_i(\langle\mu_0\mu_l\mu_i\rangle/\bar{n} - \langle\mu_0\mu_l\rangle) - 2\langle\mu_0\mu_l\rangle\sum_i(\langle\mu_0\mu_k\mu_i\rangle/\bar{n} - \langle\mu_0\mu_k\rangle) \\ &\quad + 4\langle\mu_0\mu_k\rangle\langle\mu_0\mu_l\rangle\sum_i(\langle\mu_0\mu_i\rangle/\bar{n}^2 - 1)\Bigg). \qquad (24)\end{aligned}$$

Our estimators for the correlation of the μ_i may also be introduced into equation (19) to yield a new expression for the biased estimator

$$\langle \hat{g}_n(k) \rangle = \langle \hat{g}_\mu(k) \rangle - \langle \mu_0 \mu_k \rangle / M \bar{n}^3 \tag{25}$$

which—just like equation (20)—clearly separates classical intensity noise (first term) from photon detection noise (other terms).

2.4. *Intensity statistics*

In order to make further progress, we must now specify a model distribution for the time-integrated intensities μ_i. Since typical light scattering experiments are performed with a large number of statistically independent scattering centres and coherent detection, we expect to detect quasithermal light, that is light with a complex Gaussian amplitude and negative exponential intensity statistics. In fact, such Gaussian models were used throughout the earlier calculations of estimator noise in photon correlation [2–4].

However, real experiments almost always involve significant spatial integration. In order to detect a sufficient amount of scattered light, a large detector aperture is highly desirable. The obvious conflict with the requirement of coherent detection is typically solved by choosing a detector aperture comparable to the size of one coherence area. As a result, the normalized photon correlation function shows an intercept

$$\beta = \lim_{\substack{k>0 \\ k \to 0}} \langle g_n(k) \rangle \tag{26}$$

less than one, the value expected for quasithermal light.

Probably the simplest statistical model that is able to provide arbitrary intercepts in the correlation function is the assumption of gamma statistics for the time-integrated detected intensity μ_i. Gamma distributions with scale parameter μ and shape parameter α,

$$p_\mu(\mu_i) = (\mu_i/\mu)^{\alpha-1} \exp(-\mu_i/\mu)/\mu\Gamma(\alpha) \tag{27}$$

are obtained exactly, if μ_i equals the intensity obtained by summing over α independent speckles, each with quasithermal statistics and intensity expectation μ [11]. The distribution parameters are closely related to the expectation of μ_i and the intercept β by

$$\langle \mu_i \rangle = \bar{n} = \alpha\mu \tag{28}$$

$$\beta = \mathrm{var}(\mu_i)/\bar{n}^2 = \alpha\mu^2/\alpha^2\mu^2 = 1/\alpha. \tag{29}$$

While real integrated intensities may not be exactly gamma variables [14], deviations are typically small and we shall use gamma statistics for the purpose of noise estimation throughout this paper. It should be noted that for large α the gamma distribution approaches a Gaussian. Hence the same model may be used not only for homodyne detection but also for heterodyne experiments, [1]. The exact heterodyne case is obtained by keeping the terms of lowest order in $\beta = 1/\alpha$, only.

For the evaluation of equation (20), our estimator covariance of the normalized autocorrelation function, we need mixed moments of the μ_i up to fourth order. These

moments may be calculated fairly easily by considering the gamma variable μ_i to be a sum of α absolute squares of independent complex Gaussian variables $u_j(i)$,

$$\mu_i = \sum_{j=1}^{\alpha} |u_j(i)|^2 \tag{30}$$

with normalized complex autocorrelation

$$\chi_k = \langle u_j(i) u_j(i+k) \rangle / \mu . \tag{31}$$

Using the familiar factorization rules for moments of Gaussian random variables, we obtain

$$\langle \mu_0 \rangle = \alpha\mu = \bar{n} \tag{32}$$

$$\langle \mu_0 \mu_i \rangle = \alpha(\alpha + |\chi_i|^2)\mu^2 = \bar{n}^2(1 + \beta|\chi_i|^2) \tag{33}$$

$$\langle \mu_0 \mu_i \mu_j \rangle = \bar{n}^3[1 + \beta|\chi_i|^2 + \beta|\chi_j|^2 + \beta|\chi_{i-j}|^2 + 2\beta^2 \mathrm{Re}(\chi_i \chi^*_{i-j} \chi^*_j)] \tag{34}$$

$$\begin{aligned}\langle \mu_0 \mu_i \mu_j \mu_m \rangle = \bar{n}^4[&1 + \beta|\chi_i|^2 + \beta|\chi_j|^2 + \beta|\chi_m|^2 + \beta|\chi_{i-j}|^2 + \beta|\chi_{i-m}|^2 + \beta|\chi_{j-m}|^2 \\ &+ 2\beta^2 \,\mathrm{Re}(\chi_i \chi^*_{i-j} \chi^*_j) + 2\beta^2 \,\mathrm{Re}(\chi_i \chi^*_{i-m} \chi^*_m) + 2\beta^2 \,\mathrm{Re}(\chi_j \chi^*_{j-m} \chi^*_m) \\ &+ 2\beta^2 \,\mathrm{Re}(\chi^*_{i-j} \chi^*_{j-m} \chi_{i-m}) + \beta^2|\chi_i|^2|\chi_{j-m}|^2 + \beta^2|\chi_j|^2|\chi_{i-m}|^2 + \beta^2|\chi_m|^2|\chi_{i-j}|^2 \\ &+ 2\beta^3 \,\mathrm{Re}(\chi_i \chi^*_{i-j} \chi^*_{j-m} \chi^*_m) + 2\beta^3 \,\mathrm{Re}(\chi_i \chi^*_{i-m} \chi_{j-m} \chi^*_j) \\ &+ 2\beta^3 \,\mathrm{Re}(\chi_j \chi^*_{j-i} \chi^*_{i-m} \chi^*_m)].\end{aligned} \tag{35}$$

The χ_k may now be further specified by a specific model correlation function, for example, as

$$\chi_k = \exp(-\Gamma|k|) \tag{36}$$

for light with a Lorentzian spectrum and singly exponential correlation. If we know that the χ_k are all real, they can easily be estimated from the available photon correlation data, since, ignoring bias,

$$\langle \hat{g}_n(k) \rangle = \beta|\chi_k|^2 \tag{37}$$

and we may use

$$\chi_k = [\hat{g}_n(k)/\beta]^{1/2}. \tag{38}$$

β must be estimated as the zero-lag limit of the normalized correlation. Obviously, equation (38) is of no use whenever an experimental value of the normalized correlation happens to fall below zero. The commonly used countermeasure is to assume that all χ_i vanish for all $i \geqslant k$, where k is the smallest positive integer with a normalized measured correlation less than zero. This scheme should work well enough for our purpose of noise estimation.

It should be pointed out that knowledge of all correlation channels up to the final decrease into the baseline is required for proper noise estimation. While this is generally easily achieved for processes with a single time scale, difficulties may arise with signals that contain several very different spectral components. Multiple sample time correlation may be required in this instance.

Introducing the gamma moments of equations (32)–(35) into equations (20) and (24), we obtain the final expression for the covariance matrix of the normalized photon correlation estimator,

$$\begin{aligned}\operatorname{cov}(\hat{g}_n(k),\hat{g}_n(l)) = M^{-1}\beta^2\Bigg[&\sum_i |\chi_i|^2|\chi_{i+k-l}|^2 + \sum_i |\chi_i|^2|\chi_{i+k+l}|^2 \\ &+ 2\beta\,\mathrm{Re}\Big(\chi_k\chi_l^*\sum_i \chi_i\chi_{i+k-l}^*\Big) + 2\beta\,\mathrm{Re}\Big(\chi_k\chi_l\sum_i \chi_i\chi_{i+k+l}^*\Big) \\ &+ 2\beta\,\mathrm{Re}\Big(\sum_i \chi_i\chi_{i+k}^*\chi_{i+l}^*\chi_{i+k+l}\Big) + 4\beta|\chi_k|^2|\chi_l|^2\sum_i |\chi_i|^2 \\ &- 4\beta|\chi_l|^2\,\mathrm{Re}\Big(\chi_k\sum_i \chi_i\chi_{i+k}^*\Big) - 4\beta|\chi_k|^2\,\mathrm{Re}\Big(\chi_l\sum_i \chi_i\chi_{i+l}^*\Big) \\ &+ 2\beta^{-1}\bar{n}^{-1}[|\chi_{k-l}|^2 + |\chi_{k+l}|^2 + 2\beta\,\mathrm{Re}(\chi_k\chi_{k-l}^*\chi_l^*) \\ &+ 2\beta\,\mathrm{Re}(\chi_k\chi_{k+l}^*\chi_l) - 2\beta|\chi_k|^2|\chi_l|^2] + \beta^{-2}\bar{n}^{-2}\delta_{kl}(1+\beta|\chi_k|^2)\Bigg]. \end{aligned} \tag{39}$$

The limit $\beta = 1$ corresponds to quasithermal light and agrees with the calculation of Saleh and Cardoso [4], if the terms missing in their calculation are added appropriately [5].

In the limit of small count rate, the covariance matrix is nearly diagonal with the well known Poisson-type channel variance [2]. For small β, that is close to the Gaussian intensity (!) limit, which may be used to model heterodyne experiments, the lowest order terms in β dominate equation (39) and we obtain

$$\begin{aligned}\operatorname{cov}(\hat{g}_n(k),\hat{g}_n(l)) \approx M^{-1}\beta^2\Bigg(&\sum_i |\chi_i|^2|\chi_{i+k-l}|^2 + \sum_i |\chi_i|^2|\chi_{i+k+l}|^2 \\ &+ 2\beta^{-1}\bar{n}^{-1}(|\chi_{k-l}|^2 + |\chi_{k+l}|^2) + \beta^{-2}\bar{n}^{-2}\delta_{kl}\Bigg). \end{aligned} \tag{40}$$

Please note that equation (40) involves $|\chi_i|^2$ only and we do not need to compute the square root in equation (38) in this case. Hence negative values of the normalized correlation, as they may occur, for example, for heterodyne measurements in velocimetry or mobility analysis, do not cause any problems.

As a final special case we consider the diagonal terms in equation (39), which are important as weight factors in inversion algorithms:

$$\begin{aligned}\operatorname{var}(\hat{g}_n(k)) = M^{-1}\beta^2\Bigg[& \sum_i |\chi_i|^4 + \sum_i |\chi_i|^2|\chi_{i+2k}|^2 + 2\beta|\chi_k|^2 \sum_i |\chi_i|^2 \\ & + 2\beta \operatorname{Re}\left(\chi_k^2 \sum_i \chi_i \chi_{i+2k}^*\right) + 2\beta \operatorname{Re}\left(\sum_i \chi_i \chi_{i+k}^{*2} \chi_{i+2k}\right) \\ & + 4\beta|\chi_k|^4 \sum_i |\chi_i|^2 - 8\beta|\chi_k|^2 \operatorname{Re}\left(\chi_k \sum_i \chi_i \chi_{i+k}^*\right) \\ & + 2\beta^{-1}\bar{n}^{-1}[1 + |\chi_{2k}|^2 + 2\beta|\chi_k|^2 + 2\beta \operatorname{Re}(\chi_k^2 \chi_{2k}^*) - 2\beta|\chi_k|^4] \\ & + \beta^{-2}\bar{n}^{-2}(1 + \beta|\chi_k|^2)\Bigg]. \end{aligned} \tag{41}$$

2.5. Noise on single exponential correlation

For gamma–Lorentzian light with

$$\chi_k = \exp(-\Gamma|k|) \tag{42}$$

we may use my previous evaluations of the summations in equation (40) [15]:

$$\sum_i |\chi_i|^2 = \coth(\Gamma) \qquad \sum_i |\chi_i|^4 = \coth(2\Gamma) \tag{43}$$

$$\operatorname{Re}\left(\sum_i \chi_i \chi_{i+k}^*\right) = \exp(-\Gamma|k|)[|k| + \coth(\Gamma)] \tag{44}$$

$$\sum_i |\chi_i|^2|\chi_{i+k}|^2 = \exp(-2\Gamma|k|)[|k| + \coth(2\Gamma)] \tag{45}$$

$$\operatorname{Re}\left(\sum_i \chi_i \chi_{i+k}^{*2} \chi_{i+2k}\right) = \exp(-4\Gamma|k|)[\coth(2\Gamma) - \coth(\Gamma)] + \exp(-2\Gamma|k|)\coth(\Gamma). \tag{46}$$

The full covariance matrix requires the knowledge of one extra summation,

$$\begin{aligned}\operatorname{Re}\left(\sum \chi_i \chi_{i+k}^* \chi_{i+l}^* \chi_{i+k+l}\right) = & \exp[-2\Gamma(k+l)][\coth(2\Gamma) - \coth(\Gamma)] \\ & + \exp(-2\Gamma k)[(k-l) + \coth(\Gamma)] \end{aligned} \tag{47}$$

if we assume $0 \leqslant l \leqslant k$. We obtain the covariance matrix of the normalized correlation estimator in the case of gamma–Lorentz intensity statistics to be

$$\begin{aligned}\operatorname{cov}(\hat{g}_n(k), \hat{g}_n(l)) = M^{-1}\beta^2[&\exp[-2\Gamma(k-l)][k-l+\coth(2\Gamma)]\\&+\exp[-2\Gamma(k+l)][k+l+\coth(2\Gamma)]\\&+2\beta\exp[-2\Gamma(k+l)][-(k+l)+\coth(2\Gamma)-2\coth(\Gamma)]\\&+4\beta\exp(-2\Gamma k)[k-l+\coth(\Gamma)]\\&+2\beta^{-1}\bar{n}^{-1}\{\exp[-2\Gamma(k-l)]+\exp[-2\Gamma(k+l)]+2\beta\exp(-2\Gamma k)\}\\&+\beta^{-2}\bar{n}^{-2}\delta_{kl}[1+\beta\exp(-2\Gamma k)]].\end{aligned} \tag{48}$$

The diagonal terms are again the estimator variances:

$$\begin{aligned}\operatorname{var}(\hat{g}_n(k)) = M^{-1}\beta^2\{&\coth(2\Gamma)+\exp(-4\Gamma k)[2k+\coth(2\Gamma)]\\&+2\beta\exp(-4\Gamma k)[-2k+\coth(2\Gamma)-2\coth(\Gamma)]+4\beta\exp(-2\Gamma k)\coth(\Gamma)\\&+2\beta^{-1}\bar{n}^{-1}[1+\exp(-4\Gamma k)+2\beta\exp(-2\Gamma k)]\\&+\beta^{-2}\bar{n}^{-2}[1+\beta\exp(-2\Gamma k)]\}.\end{aligned} \tag{49}$$

If the detector aperture is varied in a dynamic light scattering experiment, both β and the mean count rate are changed at the same time, with their product remaining constant at larger apertures and decreasing at apertures equal to or less than one coherence area. Since the useful amplitude of the normalized correlation function decreases in proportion to β, we consider the standard deviation of the contents of a correlation channel, that is the square root of our variance expression, divided by β, as well. This corrected standard deviation,

$$\begin{aligned}\hat{S}(k)/\beta = [\operatorname{var}\hat{g}_n(k)]^{1/2}/\beta = M^{-1/2}\{&\coth(2\Gamma)+\exp(-4\Gamma k)[2k+\coth(2\Gamma)]\\&+2\beta\exp(-4\Gamma k)[-2k+\coth(2\Gamma)-2\coth(\Gamma)]\\&+4\beta\exp(-2\Gamma k)\coth(\Gamma)+2\beta^{-1}\bar{n}^{-1}[1+\exp(-4\Gamma k)+2\beta\exp(-2\Gamma k)]\\&+\beta^{-2}\bar{n}^{-2}[1+\beta\exp(-2\Gamma k)]\}^{1/2}\end{aligned} \tag{50}$$

shows a decrease in noise with decreasing intercept β in all orders of the count rate. Hence, statistical accuracy is generally improved by the use of larger apertures. This improvement approaches $2^{1/2}$ at small lag times and vanishes at large lag times, independent of the mean count rate. The reason for the better noise performance at smaller values of β may be attributed to the pronounced reduction in higher order moments of the gamma-distributed intensity.

The corrected standard deviation, equation (50), has been plotted in figure 1 as a function of channel number k or lag time kt_s for a count rate of 10 photons per coherence time t_c and coherence area. The sample time was chosen to be $0.05\,t_c$ and 100 channels are shown. Similar pictures are obtained at smaller count rates, but the region of rising standard deviations shifts slightly towards reduced lag times.

As predicted, the plot demonstrates a noticeable improvement in signal-to-noise ratio by use of a detector aperture significantly larger than a single coherence area. The noise reduction saturates towards small β; there is little to be gained by aperture areas in excess of 10 coherence areas. In practice, other constraints, like count rate limits due to dead time or fluctuations in laser power, may impose additional limits upon the maximum aperture. However, the use of comparatively large apertures is

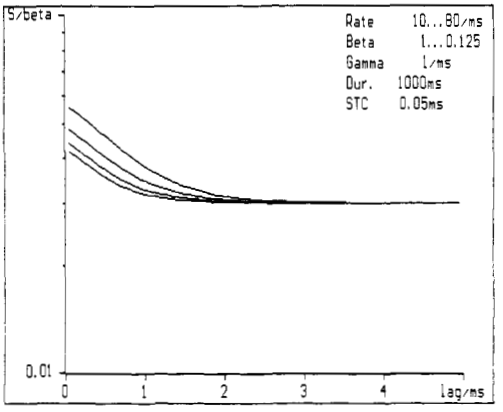

Figure 1. Corrected standard deviation as a function of lag time for intercepts $\beta = 1$, 0.5, 0.25 and 0.125 (from top to bottom at left margin).

simultaneously favourable, whenever static as well as dynamic light scattering is measured by a single instrument.

Figures 2 and 3 show parts of the full covariance matrix corresponding to equation (48) on the same scale as was already used in figure 1, which is obtained by taking the square root of the covariance and dividing by the intercept β. The experimental conditions are chosen just as for figure 1 with intercepts of 1 in figure 2 and 0.5 in figure 3.

As it is difficult to read numerical values from a pseudo-three-dimensional plot, values are plotted on a single graph for various sets of channel indices k and l. While one index is varied continuously and the corresponding lag times are given on the abscissa, the other index is varied in steps of five, only, over a range from five to fifty. The ten curves are easily identified by the characteristic photon noise peaks obtained for $k = l$.

All curves show a decay with increasing absolute differences in lag times over time scales comparable with or even larger than the coherence time. Such strongly correlated noise may easily be overlooked during the analysis of measured photon

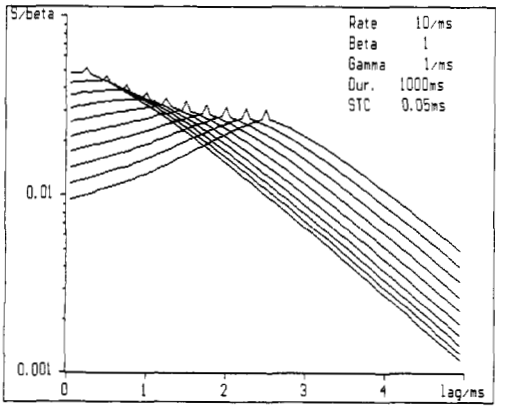

Figure 2. Corrected square root of covariance between channels 5, 10, 15, . . . , 50 (from top to bottom at left margin) and all other channels in a 100-channel correlation function for $\beta = 1$.

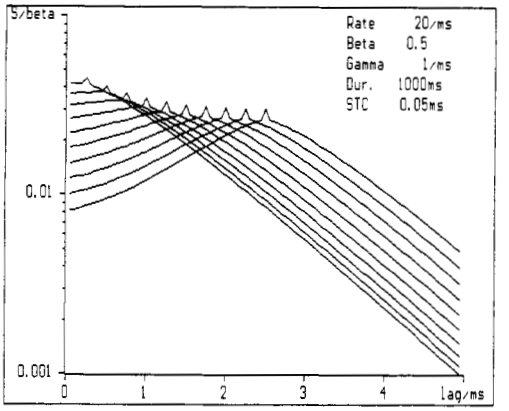

Figure 3. Corrected square root of covariance between channels 5, 10, 15, . . . , 50 (from top to bottom at left margin) and all other channels in a 100-channel correlation function for $\beta = 0.5$.

correlation functions due to its smooth character. Overfitting will be a typical consequence. With decreasing intercept, all those covariances, which involve at least one channel at small lag times, are reduced similar to the standard deviations considered above. This trend continues towards smaller intercepts and saturates again for $\beta \approx 0.1$.

At smaller count rates, we observe the expected increase in noise amplitude and a marked growth of the photon noise peaks on the diagonal of the covariance matrix. Figure 4 shows the corrected square root of the covariance for a count rate of one photon per coherence time.

3. Correlation at multiple sample times

Typical applications of photon correlation techniques in dynamic light scattering on colloidal systems require an analysis in terms of the time constants of exponential

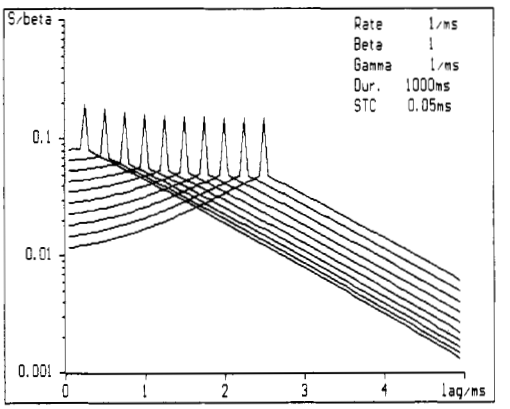

Figure 4. Corrected square root of covariance between channels 5, 10, 15, . . . , 50 (from top to bottom at left margin) and all other channels in a 100-channel correlation function for $\beta = 1$ at a reduced count rate.

contributions to the correlation function, that is Laplace inversion of the measured data. The ill-posed nature of this inversion procedure severely limits the resolution obtainable [16]. The eigenfunction analysis of the problem [17], as well as practical experience, shows that a correlogram obtained at a very large number of equally spaced lag times produces no better inversion results than a correlogram with just a few channels spaced logarithmically in lag time and covering the same total range of lag times. Especially for large lag time ranges, the second approach clearly offers identical performance at a highly reduced cost of hardware. A number of correlators with quasilogarithmic channel spacing and/or multiple sample times are now commercially available.

A second reason for the growing popularity of quasilogarithmic lag time scales is the possibility to cover extremely large lag time ranges in one single experiment. This feature is often a necessity for the analysis of strongly interacting colloids like dispersions at high concentrations and systems close to a glass transition. But it can also be very useful just as a safeguard against artefacts like afterpulsing and dead time of the photomultiplier, drifts of laser power, low-frequency vibration, or light scattered by dust in the sample.

An important feature for the construction of correlators with quasilogarithmic lag times is the use of sample time intervals that are increased in proportion to the lag time. This increase in sample time causes a proportional increase in the mean number of photons counted per sample time and thus quickly reduces the photon noise contributions to our estimator covariance expression, equation (39).

At lag times well beyond the time scale of the fastest intensity fluctuations, the sample time grows sufficiently to provide efficient averaging over these fluctuations, as well. Hence, classical noise performance can be improved, as well.

In conjunction with the novel symmetric normalization scheme, introduced above, the use of increasing sample times can finally lead to greatly enhanced accuracy in the detection of weak slow components or just be used to establish a very reliable baseline [13].

3.1. Triangular averaging

A possible problem associated with the use of multiple sample times was pointed out in the first section of this paper. The triangular averaging in equation (4) will lead to slight distortions of the measured photon correlation functions, which depend upon the sample time.

Typical correlation functions in dynamic light scattering are superpositions of negative exponentials. For one such exponential with time constant Γ, that is a normalized intensity correlation

$$g_I(\tau) = \langle I(0)I(\tau)\rangle / \langle I(0)\rangle^2 - 1 = \beta |\chi(\tau)|^2 = \beta \exp(-\Gamma\tau) \tag{51}$$

the triangular average in equation (4) results in a normalized correlation of the time-integrated intensity μ with expectation value

$$\begin{aligned} \langle \hat{g}_\mu(k)\rangle &= \beta t_s^{-2} \int_{-t_s}^{t_s} \exp[-\Gamma(kt_s + t)](t_s - |t|)\, \mathrm{d}t \\ &= \beta t_s^{-2}\Gamma^{-2}[2\cosh(\Gamma t_s) - 2]\exp(-\Gamma k t_s). \end{aligned} \tag{52}$$

It should be noted that equation (52) requires $k>0$. Series expansion for small Γt_s yields

$$\langle \hat{g}_\mu(k)\rangle \approx \beta \exp(-\Gamma k t_s)[1+\tfrac{1}{12}\Gamma^2 t_s^2+O(\Gamma^4 t_s^4)]. \tag{53}$$

We obtain a slight increase in amplitude as compared with equation (5). For $\Gamma t_s = 0.1$, this increase is less than 0.1%, justifying our previous approximation, equation (5).

A noticeable distortion occurs only at sample times t_s, which are a significant fraction of $1/\Gamma$. For a fixed ratio of lag time τ and sample time t_s, this distortion will increase with lag for $\tau > 1/\Gamma$ due to the parallel increase in the sample time t_s. However, beyond a maximum, which is easily computed as

$$\delta g(2/\Gamma) \approx \beta \exp(-2)(t_s/\tau)^2/3 \approx 0.045\,\beta(t_s/\tau)^2 \tag{54}$$

the decay of the exponential will quickly reduce the absolute amount of distortion. If we choose $t_s/\tau = \frac{1}{8}$, this error is already less than 10^{-3} and certain to be covered by noise in almost any application.

3.2. *Multiple-tau correlation*

The technical realization of varying lag and sample times is greatly simplified, if the desired logarithmic scale is replaced by an approximation based upon subsequent doubling of sample time and lag time increments every L channels ('L channels per octave'). As we have just seen, the choice of $L=8$ is sufficient to reduce triangular averaging distortions to less than 10^{-3}.

In order to obtain some correlation information at lags smaller than Lt_{s0}, where t_{s0} is the initial (smallest) sample time, it is possible to use $2L$ channels at this sample time covering lags between 0 and $(2L-1)t_{s0}$. At all other sample times t_{sj}, $j>0$, L channels with lags between Lt_{sj} and $(2L-1)t_{sj}$ provide a quasilogarithmic lag time scale of uniform average density in $\log\tau$. This scheme was named 'multiple tau' by a manufacturer of such correlators [18].

In order to apply our theory of estimator noise to 'multiple-tau' correlation functions, we must first take into account the variation of the mean photon count number per sample time interval with the sample time. The mean counts simply grow in proportion to the sample time t_{sj},

$$\bar{n}_j = 2^j \bar{n}_0. \tag{55}$$

A more subtle change occurs due to the triangular averaging over increasingly larger sample time intervals with increasing lag time. As we have just seen, there is no significant change to the expectation of the measured correlation function, as long as the ratio of sample time and lag time is sufficiently small.

However, our noise estimates involved sums over correlation values at all lags, particularly also at lag zero. At zero lag time, the triangular averaging generally introduces a reduction of the finite sample time correlation, which is due to the decay of $|\chi(t)|^2$ with $|t|$:

$$\langle \hat{g}_\mu(0)\rangle = \beta t_s^{-2} \int_{-t_s}^{t_s} |\chi(t)|^2 (t_s - |t|)\,\mathrm{d}t. \tag{56}$$

As an instructive example, we consider once again a singly exponential correlation and obtain

$$\langle \hat{g}_\mu(0)\rangle = \beta t_s^{-2} \int_{-t_s}^{t_s} \exp(-\Gamma|t|)(t_s - |t|)\,\mathrm{d}t = 2\beta\{1-[1-\exp(-\Gamma t_s)]/\Gamma t_s\}/\Gamma t_s. \tag{57}$$

Equation (57) demonstrates the 'loss in intercept' commonly observed at sample times larger than the coherence time. It should again be stressed, however, that there is no similar reduction in correlations at non-zero lags and we cannot simply modify our β to take care of triangular averaging.

Equation (56) implies the need for special consideration of sample time averaging for all χ_0 terms in our covariance expression, equation (39). A 'multiple-tau' correlation measurement provides us with estimates of $\chi(\tau)$ at all lag times of interest (that is where $\chi(\tau)$ differs significantly from zero and one), if we apply equation (38). These estimates may be used in a straightforward manner to obtain estimates for the χ_k at reasonably large k, independent of the sample time t_s. However, χ_0 should always be estimated using

$$|\hat{\chi}_0|^2 = t_s^{-2} \int_{-t_s}^{t_s} |\chi(t)|^2 (t_s - |t|)\,\mathrm{d}t. \tag{58}$$

Of course, equation (58) reduces to $|\chi(0)|^2 = 1$ for sample times well below the shortest coherence time. But a very significant reduction will typically occur at large lags, just where the χ_0 terms dominate our covariance expression. It is essentially this sample time-dependent reduction of χ_0, which causes the tremendous signal-to-noise advantage connected with increasing the sample time in proportion to the lag time.

A smaller triangular averaging effect is also present in $|\chi_1|^2$, which includes contributions down to lag zero, as well. A more precise estimate than just $|\chi(t_s)|^2$ would be

$$|\chi_1|^2 = t_s^{-2} \int_0^{2t_s} |\chi(t)|^2 (t_s - |t - t_s|)\,\mathrm{d}t. \tag{59}$$

For all higher k, triangular averaging may typically be ignored, and we may use

$$|\hat{\chi}_k|^2 = |\chi(kt_s)|^2 \qquad k > 1. \tag{60}$$

Many of the sums in our covariance expression do require a summation over all the $|\chi_k|^2$. In such sums, the triangular weights in equations (58) and (59) overlap such that they always add to yield t_s. Hence, we obtain a trivial dependence of the sum over $|\chi_k|^2$ on t_s:

$$\sum_i |\chi_i|^2 = 2t_s^{-1} \int_0^\infty |\chi(t)|^2\,\mathrm{d}t. \tag{61}$$

We do not need to consider equations (58) and (59) in this case, but should rather use equation (61) at all sample times. The integral in equation (61) is the conventional definition of the coherence time t_c.

In practice, convergence problems may arise during the computation of equation (61) if the total measurement time was not chosen sufficiently large or the measured signal was not sufficiently stationary. These situations may lead to significant measured correlation up to very large lags, which then tend to dominate the coherence time integral. Of course, the situations described lack the important prerequisite of a

stationary signal, and—strictly speaking—a correlation is simply not well defined at all. Hence, particular caution is required, whenever extremely large coherence times are predicted, particularly if these predictions also vary from one measurement run to the next.

$|\chi_i|^2$ terms appear in products with correlation coefficients at different lags, as well. As long as these other factors remain sufficiently smooth for small values of i, we may apply the same argument of triangular weight cancellation again and can still obtain reliable estimates without use of equations (58) and (59).

However, sums over other than second powers of $|\chi_i|$ do not show perfect cancellation of triangular averaging effects. This becomes particularly important for the $|\chi_i|^4$ sum, which dominates the variance expression equation (41) at large lags. A useful computation scheme for this case involves the combination of an estimate for the integral over $|\chi(t)|^4$ from $2t_s$ to infinity (that is the maximum lag or the lag with the first negative normalized correlation estimate, respectively) with equations (58) and, possibly, also (59):

$$\sum_i |\chi_i|^4 = (|\hat{\chi}_0|^2)^2 + 2(|\hat{\chi}_1|^2)^2 + 2t_s^{-1} \int_{2t_s}^{\infty} |\chi(t)|^4 \, dt. \tag{62}$$

For large lags, only the first term in equation (62) contributes and yields $(2t_c/t_s)^2$. Hence, even after division by M, the number of samples, which is of order t_s^{-1}, there remains a decrease in estimator variance for the normalized correlation function of order t_s. This result supports my earlier claim of the importance of increasing the sample time in proportion to the lag time for 'multiple-tau' correlators.

With the scheme sketched above, we can calculate the covariance matrix for multiple sample time correlation functions at all lag times. However, our theory does not really apply at very large lags. If the lag time becomes a significant fraction of the total duration of the measurement, our assumption of a large number of samples will eventually fail, and special consideration of boundary effects is required.

In this case we are, however, also in the regime where symmetric normalization significantly reduces estimator noise. This reduction is essentially due to a cancellation of all boundary contributions [13]. Hence, the validity of our previous calculations in the region of very large lags is re-established if we use the symmetrically normalized correlation estimator $g_n^{(s)}(k)$ of equation (9) in place of $g_n(k)$.

3.3. Multiple-tau correlation of single exponential

In order to illustrate the general behaviour of our noise expression for multiple-tau measurements, we focus our attention, once again, on data with a singly exponential temporal autocorrelation. Figure 5 shows the corrected standard deviation, that is the square root of the estimator variance divided by the intercept β, for a 'multiple-tau' correlator with an initial sample time of 200 ns and $L = 8$ 'channels per octave'. The intercept is kept at one and the count rate is varied over five decades.

At very low count rates, photon noise dominates up to lag times well beyond the coherence time. Decreases in estimator standard deviation equal to $\sqrt{2}$ at every doubling of the sample time are typical in this regime. Only for very large lags, is photon noise averaged below the small classical noise contribution and then our standard deviation saturates. At these large lags, noise is governed by the cross term between photon and classical noise, the term linear in reciprocal count rate in our

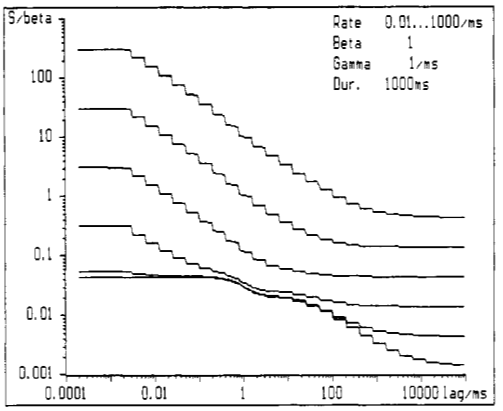

Figure 5. Corrected standard deviation for a 'multiple-tau' correlator operating at lag times between 200 ns and 100 s, for $\beta = 1$ and count rates per coherence time of 0.01, 0.1, 1, 10, 100 and 1000 (from top to bottom).

variance expression, equation (41). Consequently, the plotted standard deviation shows a large lag limit, which is proportional to the inverse square root of the count rate.

With increasing count rate, the saturation time decreases. At about 10 photons per coherence time, this decrease is down to the coherence time and classical noise starts to dominate. As is well known, no significant further noise reductions are possible at lags close to the coherence time. However, the statistial accuracy at both, smaller as well as larger lag (and sample!) times, may still be improved by further increases in the mean count rate. This may be an important advantage, if other, possibly much weaker, spectral components are present at either very short or very large times.

For large count rates, the predicted noise amplitude remains almost constant towards smaller lag and sample times. This is due to the dominance of classical noise. Due to its high degree of covariance across all small lag time channels, this presence of classical noise is not easily spotted in a single experiment. In contrast, the—really considerably smaller—photon noise contribution, which still increases towards smaller sampling times, is immediately visible as a random scatter in the graph of measured correlation functions.

Repetitions of the experiment should reveal the presence of classical noise as a noticeable fluctuation in measured values of the intercept β.

The dependence of the corrected estimator standard deviation upon intercept is very similar to what we observe in the single sample time situation. Figure 6 demonstrates the decrease in noise at lags below the coherence time due to the reduced intercepts.

4. Conclusions

Most experiments in dynamic light scattering involve scattering from a large number of particles, which results in Gaussian field amplitudes at the detector. Light detected through a finite-size aperture is then well described as a stochastic process with gamma intensity statistics. The estimator covariance for the corresponding normalized photon

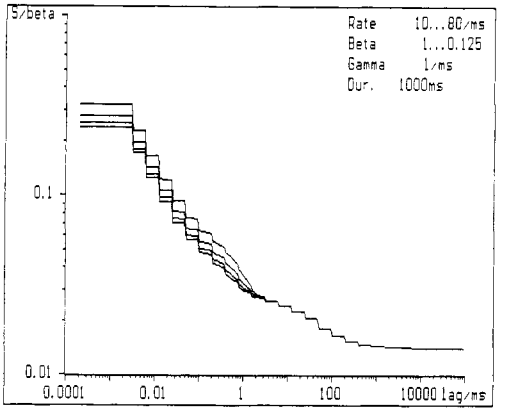

Figure 6. Corrected standard deviation for a 'multiple-tau' correlator operating at lag times between 200 ns and 100 s, for $\beta = 1, 0.5, 0.25$ and 0.125, and the corresponding count rates per coherence time of 10, 20, 40 and 80 (from top to bottom).

autocorrelation function was computed. At count rates close to and above some 10 photons per coherence time and coherence area, noise on measured photon correlation functions is largely due to classical intensity fluctuations and very highly correlated over lag time ranges in excess of the coherence time. This type of noise is not readily visible on measured data and will very likely lead to overfitting by common evaluation programs.

If the simultaneous variation in intercept is taken into appropriate account, noise estimates may be compared for various detector apertures. With increasing detector aperture, the probability density of intensity fluctuations changes from exponential to Gaussian. As a consequence of this change, we observe a decrease in higher order relative moments, which reduces the estimator variance for the photon correlation function by a factor up to two for lag times shorter than the coherence time. A noticeable improvement is possible in terms of signal-to-noise ratio, if the detector aperture is increased to about 10 coherence areas.

For photon correlation data measured with multiple-tau instruments, noise estimation requires the consideration of triangular averaging effects. As a result of our calculations we find a marked decrease in noise with increasing count rate at very short and very large lag times, even if the count rate exceeds the 'magic value' of about 10 photons per coherence time and coherence area. In order to realize the possible improvements in signal-to-noise towards large lags, it is of fundamental importance to implement a sampling time that increases in proportion to the lag time and to use a symmetric normalization scheme.

References

[1] Schätzel K 1986 Correlation techniques in dynamic light scattering *Appl. Phys.* B **41** 193–213
[2] Jakeman E, Pike E R and Swain S 1971 Statistical accuracy in the digital autocorrelation of photon counting fluctuations *J. Phys. A: Gen. Phys.* **4** 517–34
[3] Degiorgio V and Lastovka J B 1971 Intensity–correlation spectroscopy *Phys. Rev.* A **4** 2033–50
[4] Saleh B E A and Cardoso M F 1973 The effect of channel correlation on the accuracy of photon counting digital autocorrelators *J. Phys. A: Math. Nucl. Gen.* **6** 1897–909

[5] Kojro Z 1990 Influence of statistical errors on size distributions obtained from dynamic light scattering data. Experimental limitations in size distribution determination *J. Phys. A: Math. Gen.* **23** 1363–83
[6] Provencher S W 1982 CONTIN: A general purpose constrained regularization program for inverting noisy linear algebraic and integral equations *Comput. Phys. Commun.* **27** 229–42
[7] Livesey A K, Licinio P and Delaye M 1986 Maximum entropy analysis of quasi elastic light scattering from colloidal dispersions *J. Chem. Phys.* **84** 5102
[8] Schätzel K 1985 *New Concepts in Correlator Design 1985 (Inst. Phys. Conf. Ser. 77)* (Bristol: Institute of Physics) pp 175–84
[9] Schätzel K, Kalström R, Stampa B and Ahrens J 1989 Correction of detection-system dead-time effects on photon correlation functions *J. Opt. Soc. Am.* B **6** 937–47
[10] Schätzel K 1986 Dead time correction of photon correlation functions *Appl. Phys.* B **41** 95–102
[11] Saleh B E A 1978 *Photoelectron Statistics (Springer Series in Optical Sciences 6)* (Berlin: Springer)
[12] Oliver C J 1979 Spectral analysis with short data batches *J. Phys. A: Math. Gen.* **12** 591–617
[13] Schätzel K, Drewel M and Stimac S 1988 Photon correlation measurements at large lag times: improving statistical accuracy *J. Mod. Optics* **35** 711–8
[14] Goodman J 1985 *Statistical Optics* (New York: Wiley)
[15] Schätzel K 1983 Noise in photon correlation and photon structure functions *Opt. Acta* **30** 155–66
[16] Stock R S and Ray W H 1985 Interpretation of photon correlation spectroscopy data: a comparison of analysis methods *J. Polym. Sci. Polym. Phys.* **23** 1393–447
[17] McWhirter J G and Pike E R 1978 On the numerical inversion of the Laplace transform and similar Fredholm integral equations of the first kind *J. Phys. A: Math. Gen.* **11** 1729–45
[18] *ALV-3000 User's Manual* 1986 ALV Laser-Vertriebsgesellschaft mbH, Langen, FRG; *ALV-5000 Reference Manual* 1989